Anticorrosion Performance of *Syzygium Cumini* Leaves Extract for Carbon Steel Immersed in a Hydrochloric Acid Medium

T. Raja[1], S. S. Syed Abuthahir[1*] and K. Vijaya[2]

[1]*PG and Research Department of Chemistry, Jamal Mohamed College (Autonomous, affiliated to Bharathidasan University), Tiruchirappalli, Tamilnadu, India*
[2]*Department of Chemistry, PSNA College of Engineering and Technology (Autonomous, affiliated to Anna University), Dindigul, Chennai, Tamilnadu, India*
*Corresponding author: syedchemjmc@gmail.com

Received 15/10/2022; accepted 15/01/2023
https://doi.org/10.4152/pea.2024420302

Abstract
IE(%) of SCLAE on CR of CS immersed in 1 N HCl was herein assessed by WL method. The former increased and the latter decreased in the solution with higher Ct of SCLAE. The inhibitor blocked MS corrosion active sites, and created a protective layer that covered its surface. Pc constituents of SCLAE allowed the interaction between their hetero atoms and the metal ions from the CS surface, hindering its corrosion. Elc studies were herein used to confirm the formation of a protective layer on the CS surface. They were further reinforced by surface analysis techniques, such as FTIR and SEM. EDAX was used to analyze the elements present on the CS surface, after its immersion in 1 N HCl without and with SCLAE. R_a of polished, corroded and inhibited CS surfaces was analyzed by SEM and AFM.

Keywords: AFM, corrosion, CS, EDAX, FTIR, HCl, IE (%), SCLAE, SEM and WL method.

Introduction•

Corrosion is the gradual destruction of metals and alloys by chemical and Elc reactions with their environment. It is the process of slowly metals dissolution by gas and water vapors in the atmosphere, due to the formation of certain compounds, such as oxides, sulphides and carbonates [1-2].

Corrosion consequences are many and varied, and their effects on the safe, reliable and efficient operation of equipment or structures are often more serious than simple metal mass loss. Failures of various kinds and the need for expensive replacements may occur, even when the amount of metal destroyed is quite small [3-4].

CS is used for making alloys in structural and industrial applications, and it became paramount since the industrial revolution. Crude oil refining is carried out in several aggressive conditions that cause equipments surface corrosion. Generally, materials in contact with acid undergo corrosion, which is inevitable, and must be prevented.

• The abbreviations and symbols definition lists are in pages 186-187.

CS is also used structurally in buildings, bridges, axles, gears, shafts, rails, pipelines, couplings, cars, fridges and washing machines. High CS has a much better tensile strength, so it is used to make cutting tools, blades, punches, dies, springs and high-strength wire. New high strength alloys usually are more susceptible to a certain type of corrosive attack. The acids used as media in CS corrosion studies have become important, due to their industrial applications, such as pickling, industrial cleaning, descaling, oil recovery and petrochemical processes [5-6].

The use of inhibitors is found to be one of the most practical methods for protection against corrosion. They are used in industries to control metal dissolution, especially in acidic, neutral and basic environments. Most of the efficient CI used in industry are organic compounds that possess at least one functional group, which is considered the active center for the adsorption onto the metal surfaces.

Several researchers made an attempt to study various organic compounds as CI of Cu and Al alloys, MS, CS and composites in acids, alkaline and neutral media [7-12].

Most well-known CI are organic compounds containing hetero atoms, such as O, N, S and multiple bonds. They are not only expensive, but also toxic to both human beings and environments. Since their use as CI is limited, efforts have been made to develop cost-effective and non-toxic alternatives. Plant extracts, i.e. green inhibitors, are considered incredibly rich sources of environmentally acceptable CI.

The main goal of the present study was to evaluate IE(%) of SCLAE on the corrosion of CS immersed in 1 N HCl. IE(%) effect of SCLAE on CR of MS was calculated by WL method. CI mechanistic aspects were determined by Elc studies, such as ACIS and PDP. The protective layer formed over the CS surface was analyzed by FTIR spectroscopy technique. R_a of polished, corroded and inhibited CS was characterized by SEM. EDAX was used to analyze elements present on the CS surface after immersion in 1 N HCl, without and with SCLAE. The CS surface film R_a was characterized by AFM.

Materials and methods

CS specimens (C: 2.0%, S: 0.026%; P: 0.06%, Mn: 0.4% and Fe as the remainder), with the dimensions 1.0 × 4.0 × 0.2 cm, were polished to mirror finish, degreased with acetone, and used for WL method. The acidic solution was prepared by diluting 1 N HCl analytical grade with double distilled water.

Stock solutions preparation

Double distilled water was used wherever necessary in the solutions preparation. Analytical grade HCl was diluted to the required Ct. SCLAE was prepared by the Soxhlet extraction method. About 100 g powdered SCL were uniformly packed into a thimble and extracted with 1000 mL double distilled water. The extraction process ended when the solvent in the extractor siphon tube became colorless. Then, the extract was kept overnight for cooling, and made up to 1000 mL with the same double distilled water, in order to obtain 10% (w/v) SCLAE. Using this stock solution, different Ct of SCLAE were prepared.

WL method

WL measurements were done according to the described method [12-13], for 3 h, by immersing the CS specimens in 1 N HCl without and with SCLAE, at different Ct (2, 4, 6, 8 and 10%). After the elapsed time, CS specimens were taken out, washed, dried and weighed accurately.

IE (%) was determined by the following equation:

$$IE\ (\%) = \frac{W_0 - W_i}{W_0} \times 100 \qquad (1)$$

where W_i and W_0 are WL values (g) for CS in HCl with and without SCLAE, respectively.

CR determination

CS specimens weighed in triplicate were suspended by means of glass hooks in 100 mL 1 N HCl without and with SCLAE, at various Ct, for 3 h IT. Then, they were taken out, washed in running water, dried and weighed. From the change in the samples weight, CR values were calculated using the following relationship:

$$CR\ (mdd) = 53.5 \times WL/a \times IT \qquad (2)$$

where a is CS specimen area in cm^2.

Elc techniques

PDP study

CHI-Elc workstation, with a 660A impedance model, was used to record Elc studies. A conventional three electrode cell, with CS as WE, SC as RE and Pt as CE, was used. In every measurement, a fresh WE was used. The CS specimen was machine-cut into coupons with the dimensions 5 × 1 × 0.2 cm, and embedded in araldite (epoxy resin), leaving a 1 cm^2 surface area exposed for Elc measurements. This exerted a uniform E field on the CE. The WE and CE were immersed in 1 N HCl without and with SCLAE [14]. SC was connected to the test solution through a salt bridge. E vs. log I plots were recorded. Elc parameters, such as E_{corr}, I_{corr}, β_a and β_c, were determined from E vs. log I plots.

AC impedance measurements

Impedance spectra were used over the frequency range from 100 to 100000, with an AC signal amplitude of 0.005 V. The measurements were recorded after the electrode reached a steady E_{corr}. The experiments were carried out at a constant T of 30 ºC. An interval from 5 to 10 min was given for the system to attain a steady state OCP. Then, an AC E of 10 mV was superimposed. AC frequency was varied from 100 KHz to 100 MHz. The real (z') and imaginary (z") parts of the cell impedance were measured in ohms for various frequencies. C_{dl} values were calculated using the following relationship [15]:

$$C_{dl} = \frac{1}{2 \text{ x } 3.14 \text{ x } R_t \times f_{max}} \qquad (3)$$

Surface examination techniques

CS specimens were immersed in solutions without and with SCLAE, for 3 h. Then, they were taken out and dried. The nature of the layer formed on the CS specimens surface was analyzed by various analyses techniques.

Surface analysis by FTIR spectra

The layer formed on the CS surface was carefully removed and mixed thoroughly with KBr pellets. FTIR spectra were recorded in a Perkin–Elmer 1600 spectrophotometer, with a resolving power of 4 cm^{1}. After an IT of 3 h in various media, the specimens were taken out of the test solutions and dried. The layer formed on the CS surface was carefully scratched and thoroughly mixed, so as to make it uniform [16].

SEM studies

CS specimens immersed in the HCl solution without and with SCLAE, for 3 h, were removed, rinsed with double distilled water, dried and examined through a SEM (JEOL MODEL JSM 6390), to assess their surface morphology [17].

EDAX studies

CS specimens immersed in the HCl solution without and with SCLAE, for 3 h, were removed, rinsed with double distilled water, dried and examined by a computer controlled EDAX (Brucker Nano, GMBH, Germany), to study the elements present on their surface [18].

AFM characterization

CS specimens immersed in the HCl solution without and with SCLAE, for 3 h, were removed, rinsed with double distilled water, dried and subjected to surface examination [19]. CS surface morphology measurements were carried out by AFM, using a Veeco di Innova SPM with the software version V7.00, at the SR of 0.7 Hz.

Results and discussion

IE(%) of SCLAE and CR of CS were determined by the WL method, before and after immersion in 1 N HCl, and their values are given in Table 1.

Table 1: CS immersed in 1 N HCl without and with SCLAE, at different Ct, and IE(%) assessed by WL method.

Ct(%) of SCLAE	CR (mdd)	IE(%)
Blank	317.40	-
2	142.67	55.10
4	74.90	76.40
6	64.20	79.77
8	49.93	84.27
10	17.83	91.38

It was seen that 10% SCLAE gave 91.38% IE(%). Higher Ct of SCLAE increased its corrosion IE(%), due to the wider θ, which hold back CS dissolution. The interaction between hetero atoms present in SCLAE Pc constituents and metal ions from the CS

surface gave higher IE(%). The presence of many Pc constituents in SCLAE allowed for the CI of CS [20].

Elc analysis

Elc techniques were used for determining CR of CS. They allowed quickly assessing IE(%) and surface layer durability of SCLAE. They were used to know whether SCLAE acted as cathodic or anodic inhibitor, or both, against CS corrosion in 1 N HCl. They were also used to frame a suitable mechanism for SCLAE action on CS corrosion.

PDP study analysis

PDP technique was utilized to assess the development of a protective layer on the CS surface [21-23]. If a protective film is developed on the CS surface, LPR values increase and I_{corr} decreases. PDP arcs of CS immersed in 1 N HCl without and with SCLAE are shown in Fig. 1.

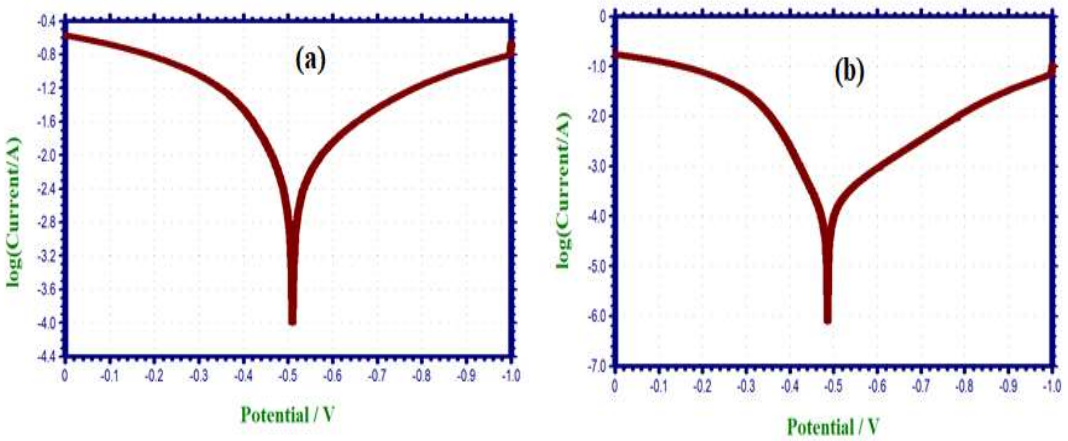

Figure 1: PDP arcs for CS corrosion in: **a)** 1 N HCl (blank); **(b)** 1 N HCl with 10% SCLAE.

Corrosion parameters, namely, E_{corr}, β_c, β_a, LPR and I_{corr}, are given in Table 2.

Table 2: PDP parameters for CS corrosion in 1 N HCl without and with SCLAE.

Ct(%) of SCLAE	E_{corr} mV/SCE	β_a mV/dec	β_c mV/dec	I_{corr} A/cm^2	LPR Ω/cm^2
blank	- 510	5.949×10^{-3}	130	181	5.5
10	- 492	1.002×10^{-3}	094	181	27.1

When CS was immersed in 1 N HCl, the following values were obtained (Fig. 1a): E_{corr} was -510 mV vs. SCE; LPR was 5.5 ohm/cm^2; and I_{corr} was 5.949×10^{-3} A/cm^2. E_{corr} shifted to the anodic side (-492 mV/SC) (Fig. 1b), when 10% SCLAE were added to 1 N HCl, due to the formation of a protective layer on the CS surface. This film controlled CS dissolution anodic reaction, by forming a Fe^{2+}/SCLAE

complex on the anodic site [24]. SCLAE acted as an anodic inhibitor, because E_{corr} shift was more negative than that of the blank solution. An increase in LPR and a decrease in I_{corr} values indicate that the inhibitor system had a more corrosion resistant nature.

ACIS results analysis

Elc impedance spectra were used to validate the development of a protective layer on the CS surface [25-27], showing that R_{ct} increased, C_{dl} decreased, and the impedance log (z/ohm) rose. AC impedance parameters, namely, R_{ct} and C_{dl}, are given in Table 3.

Table 3: Elc impedance parameters from Nyquist plots for the corrosion of CS immersed in 1 N HCl without and with SCLAE.

Ct(%) of SCLAE	Nyquist plot		Impedance log (z/ohm)	Phase angle (degree)
	R_t Ω/cm^2	C_{dl} F/cm^2		
blank	6.72	1.1082×10^{-5}	0.845	33
10	36.016	6.0593×10^{-5}	1.569	54

When CS was immersed in 1 N HCl, R_{ct} was 6.72 ohm/cm^2 and C_{dl} was 1.1082×10^{-5} F/cm^{-2}. R_{ct} value increased to 36.016 ohm/cm^2, when 10% SCLAE was added to 1 N HCl. C_{dl} value also decreased to 6.0593×10^{-5} F/cm^{-2}. Impedance value [log (z/ohm)] increased from 0.845 to 1.5698. Furthermore, the inhibitor system phase angle increased from 33.0 to 54.0°, when compared to the blank solution. This suggests that a protective layer was formed on the CS surface.

ACIS of CS immersed in 1 N HCl without and with SCLAE is shown in Figs. 2 (Nyquist plots), 3 and 4 (Bode plots).

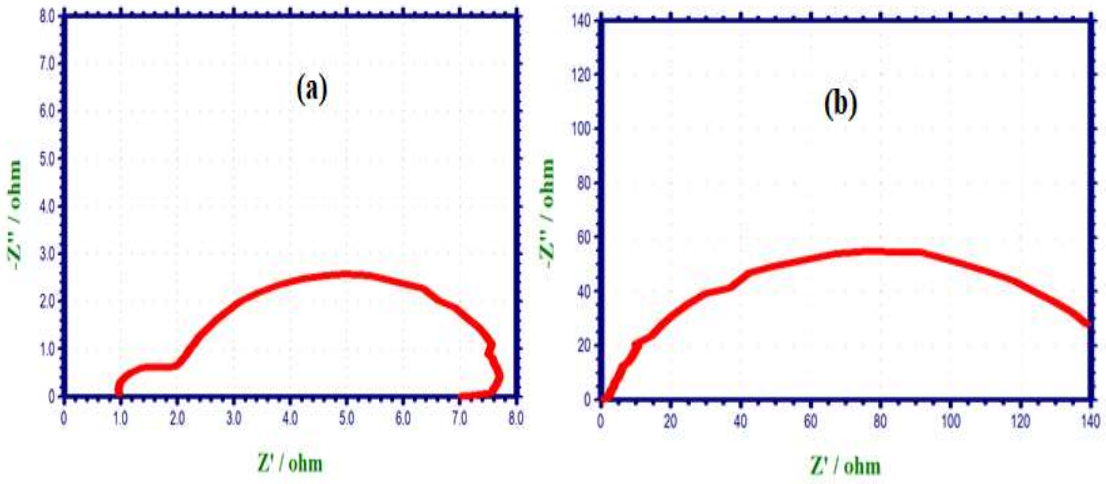

Figure 2: ACIS of CS immersed in 1 N HCl (Nyquist plots): **(a)** blank; **(b)** with 10% SCLAE.

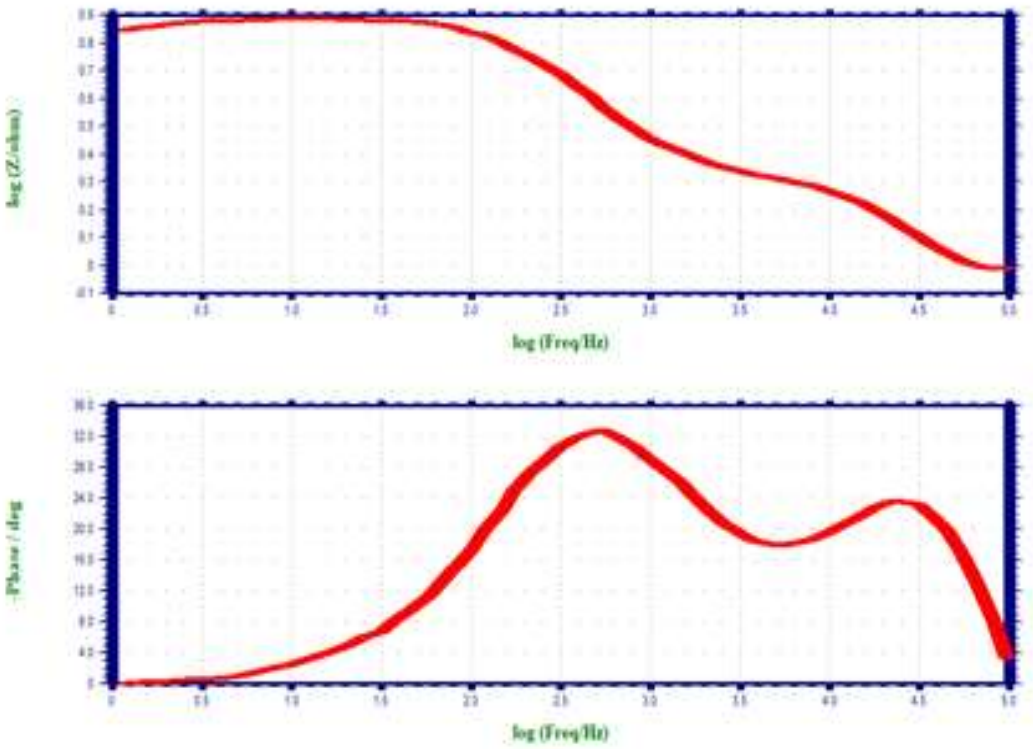

Figure 3: ACIS of CS immersed in 1 N HCl (Bode plot).

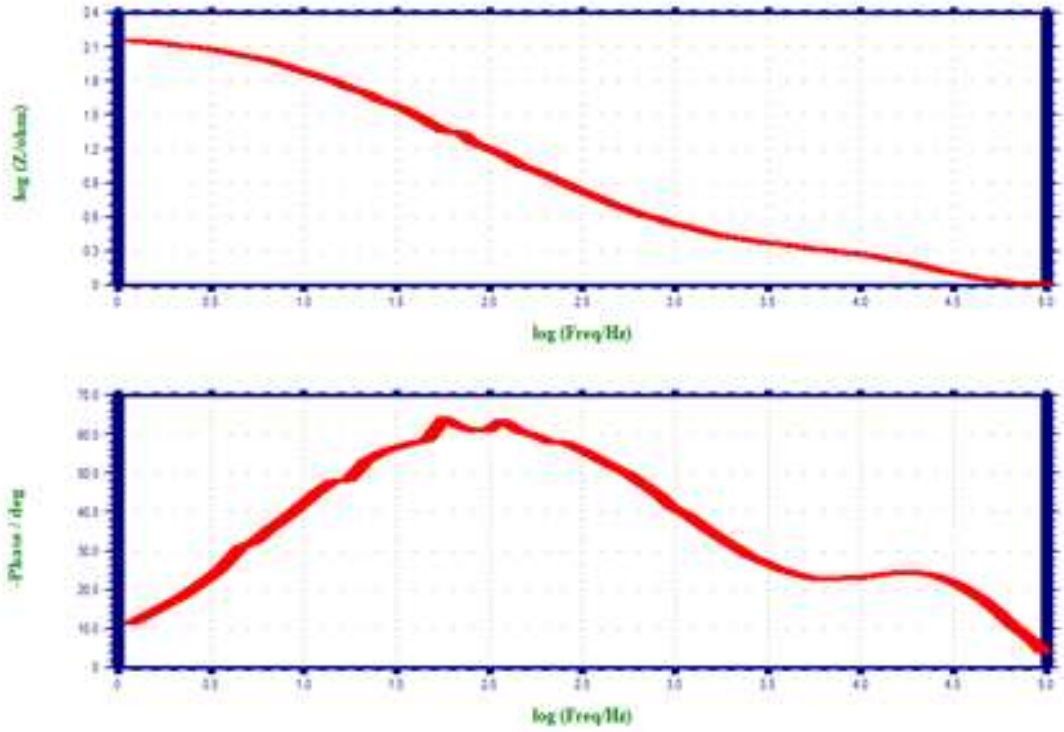

Figure 4: ACIS of CS immersed in 1 N HCl with 10% SCLAE (Bode plot).

FTIR spectra analysis

FTIR examination helps to identify absorption bands for functional groups, and inhibitor molecules alignment on the CS surface. Many researchers have reported that FTIR characterization is a major tool that can be used to predict the bonding nature of Pc constituents with the CS surface. The functional groups absorption bands in the corresponding systems are given in Table 4.

Table 4: FTIR spectral data for SCLAE, and scratched layer from the CS surface after immersion in 1 N HCl with 10% inhibitor system.

SCLAE IR bands	IR bands of the protective layer on the CS surface	Frequency assignment to functional groups
3435.98	3433.90	-OH
2923.77	2923.23	C-H stretching
1642.04	1647.02	C=O stretching
1024.96	1023.63	C-C stretching
1384.38	1385.35	C-N
681.80	603.99	N-H
-	469.89	Y-Fe_2O_3

FTIR spectrum of SCLAE is shown in Fig. 5. The peaks due to OH, C-N, C-H, C-C, C=O and N-H stretching frequencies appear at 3435.98, 1384.38, 2923.77, 1024.96, 1642.04 and 681.80 cm^{-1}, respectively [28-29].

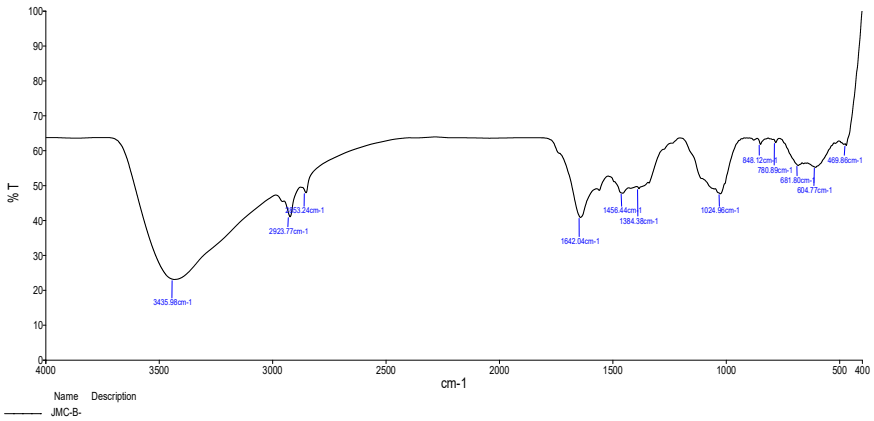

Figure 5: FTIR spectrum of SCLAE.

A protective layer was developed on the CS surface immersed in 1 N HCl with 10% SCLAE (Fig. 6). Shifts occurred in the stretching frequencies from the following functional groups: O-H, from 3435.98 to 3433.90 cm^{-1}, which indicates that molecular adsorption possibly occurred through it; C-N, from 1384.38 to 1385.35 cm^{-1}; C-H (in the pure IR spectra of SCLAE, and in the protective layer formed over the CS surface), from 2923.77 to 2923.23 cm^{-1}; C=O, from 1642.04 to 1647.02 cm^{-1}; N-H, from 681.80 to 603.99 cm^{-1}; and C-C, from 1024.96 to 1023.63 cm^{-1}. The band at 469.89 cm^{-1} mainly originated from the Fe-complex [30-31]. Almost all the band peaks appeared in SCLAE and in the

protective layer developed on the CS. This suggests that Pc constituents of SCLAE molecules adsorbed onto the MS surface. All abovementioned bands represent the formation of a complex on the alloy surface.

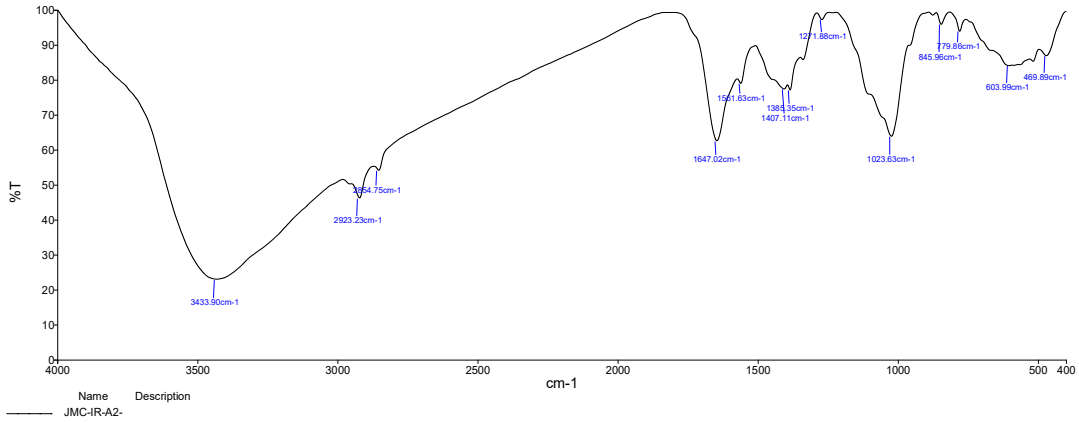

Figure 6: FTIR spectrum of a scratched layer from the CS surface after immersion in 1 N HCl with 10% SCLAE.

CS surface SEM analysis

SEM pictures of the CS surface, without and with SCLAE, were examined [32], to understand the nature of the coating developed on the alloy surface. SEM images of CS specimens immersed in 1 N HCl, for 3 h, without and with SCLAE, are shown in Fig. 7 (a, b and c).

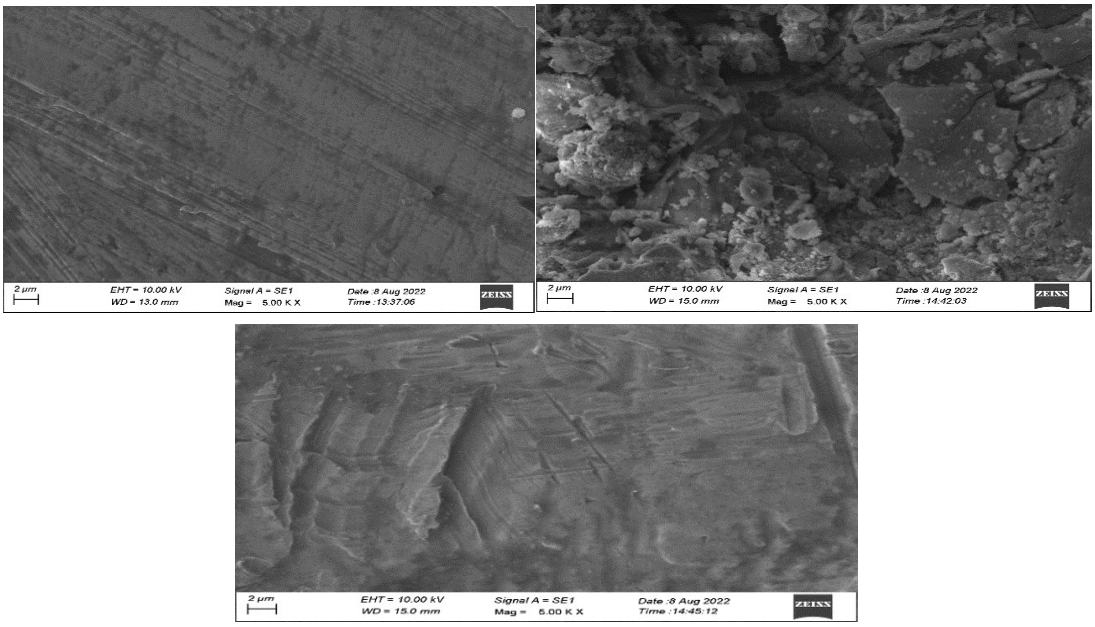

Figure 7: SEM image of polished CS coupons: **(a)** before immersion; **(b)** after immersion in 1 N HCl (blank); **(c)** after immersion in 1 N HCl with 10% SCLAE.

Fig. 7a shows CS (control) smooth surface. In Fig. 7b, CS has a rough surface with a highly corroded area, due to its dissolution in 1 N HCl (blank). Fig. 7c shows the CS surface decrease in corroded areas, since CR was suppressed in 1 N HCl with 10% SCLAE. CS is almost free from corrosion, due to the formation of an insoluble complex on its surface. The alloy R_a is almost equal to the one from the polished CS surface, since it was covered by a thin inhibitor layer that effectively controlled its dissolution [33-34].

CS surface characterization by EDAX analysis

EDAX examinations of the CS surface were performed in HCl without and with the inhibitor system. EDAX spectra were used to determine the elements present on the CS surface before and after immersion in HCl with SCLAE [35].

EDAX spectrum (Fig. 8) shows the characteristic peaks of some of the elements constituting the CS sample.

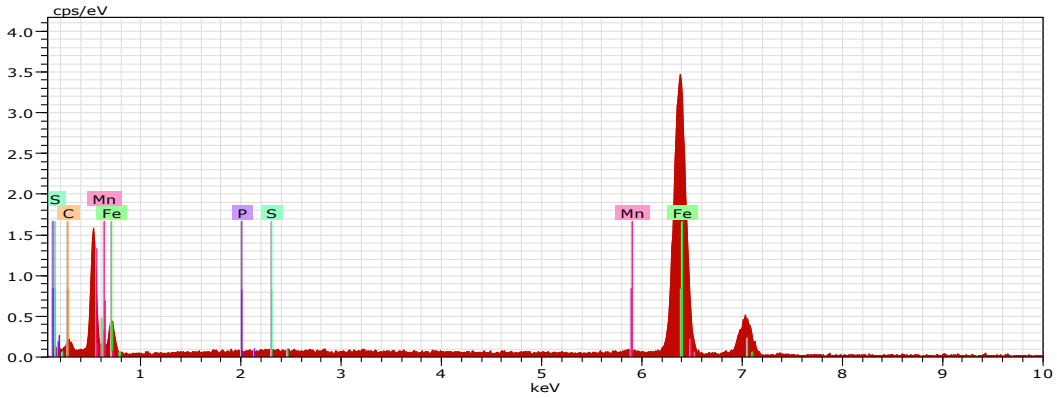

Figure 8: EDAX spectrum of CS specimen (control).

EDAX spectrum of CS immersed in 1 N HCl (Fig. 9) shows the decrease in C elements.

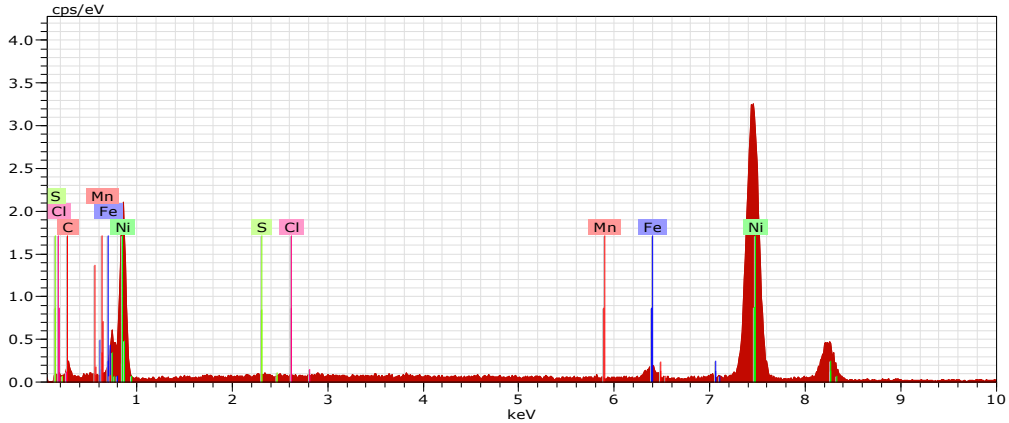

Figure 9: EDAX spectrum of CS specimen immersed in 1 N HCl (blank).

Cl^- presence indicates CS was damaged by 1 N HCl. EDAX spectrum of CS immersed in 1 N HCl with 10% SCLAE (Fig. 10) shows: a reduction in the additional line characteristic of Cl^- signals intensity; and an increase in the signal intensity of CS constituents. Fe signal appearance and O signal enhancement were due to SCLAE. These data show that the CS surface was covered with Fe, S, C, P, Ni and O atoms, due to SCLAE addition to HCl. Fig. 7c shows that Fe peaks observed in 1 N HCl with SCLAE were considerably lower than those seen in the blank solution. These results suggest that O, N and C atoms of the 10% SCLAE layer were adsorbed onto the CS surface, protecting it against corrosion, and resulting in the formation of a Fe^{2+}-SCLAE complex [36-37].

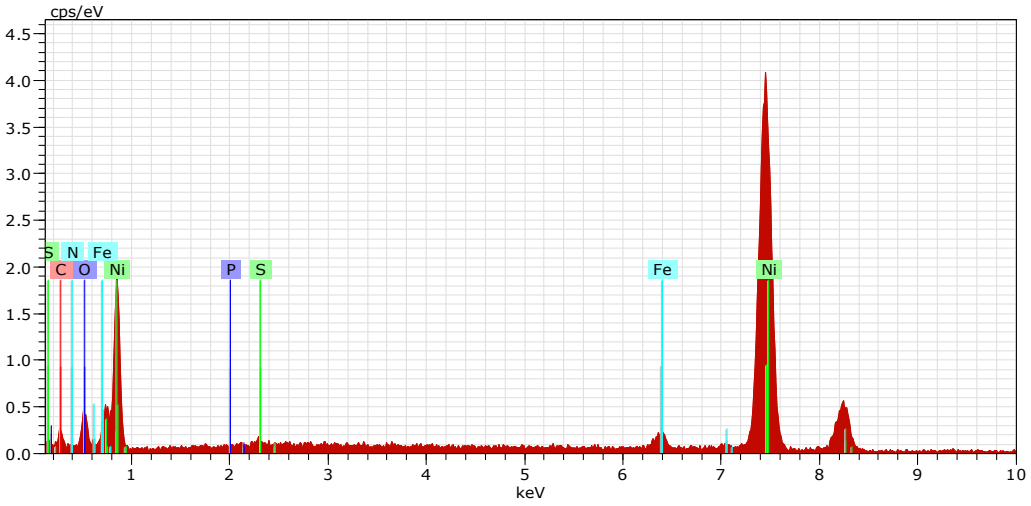

Figure 10: EDAX spectrum of CS specimen immersed in 1 N HCl with 10% SCLAE.

AFM results analysis

In any surface, roughness is easily investigated by AFM studies. AFM is a powerful tool for gathering roughness statistics from a variety of CS surfaces. It provides direct insight into the changes in the surface morphology that take place at several hundred nanometers. Topographical changes occur between the corrosion process and the formation of a protective layer on the CS surface, without and with inhibitors, respectively. In this study, AFM assessed SCLAE effect on the CS surface immersed in HCl [38-39].

This characterization comprised 3D AFM morphologies and a cross-sectional profile for the polished (control sample) CS surfaces and for those immersed in blank 1 N HCl and with 10% SCLAE (Figs. 11, 12 and 13, respectively).

AFM gave: R_a surface area; S_a (average deviation of all points roughness profile from a mean line over the evaluation length); RMS surface R_a, S_q (the average of the measured height deviations taken within the evaluation length, and measured from the mean line); S_y (the largest single P/V height in five adjoining sampling heights); and S_p maximum profile peak height (which indicates the point along the sampling length at which the curve is highest).

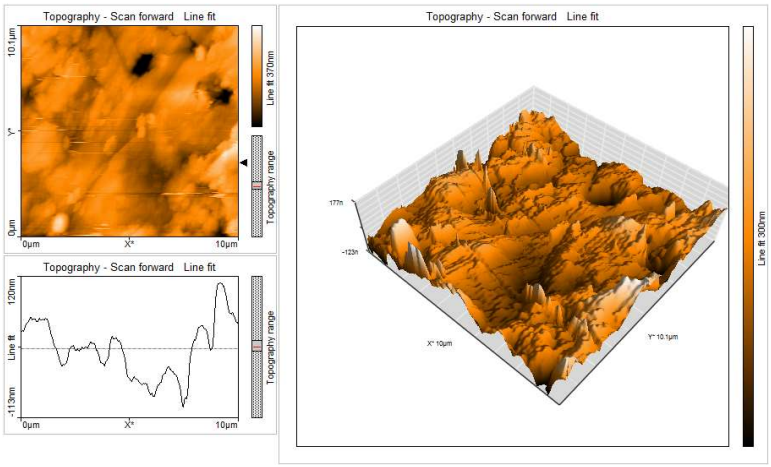

Figure 11: AFM cross sectional image of the polished CS surface (control).

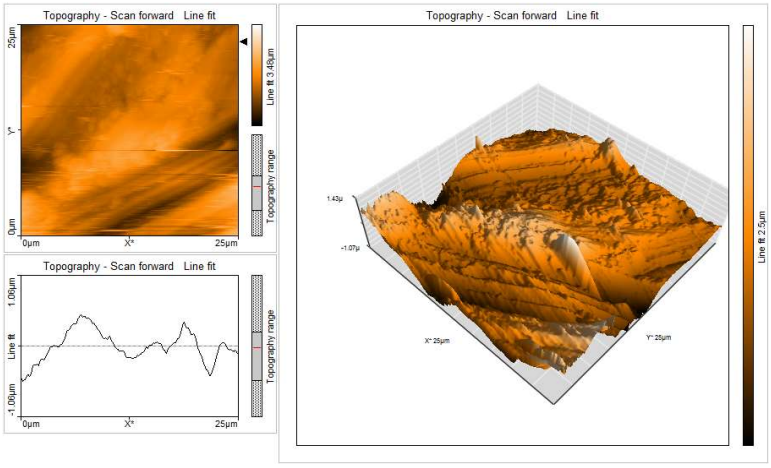

Figure 12: AFM cross sectional image of the CS surface after immersion in 1 N HCl (blank).

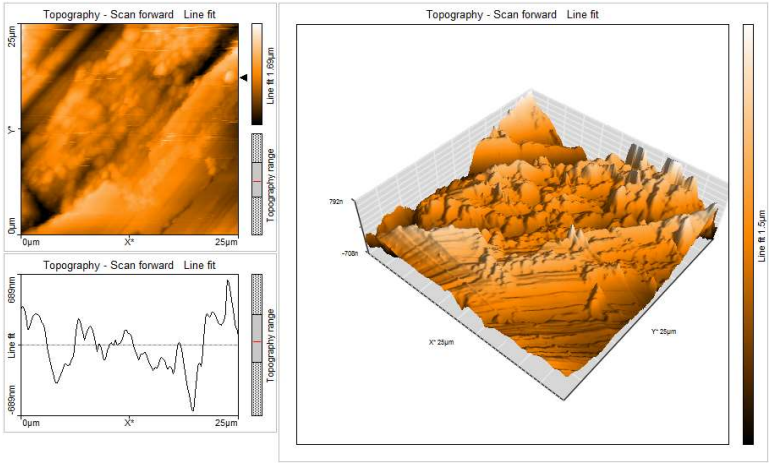

Figure 13: AFM cross sectional image for the CS surface after immersion in 1 N HCl with 10% SCLAE.

AFM parameters are given in Table 5.

Table 5: AFM data for CS immersed without and with inhibitor systems (surface area R_a).

Samples	S_a nm	S_q nm	S_y nm	S_p nm
CS surface	31.44	42.38	495.40	225.76
CS surface immersed in 1 N HCl	273.72	348.79	3334.00	1507.10
CS surface immersed in 1 N HCl + 10% SCLAE	190.55	240.11	1842.40	979.34

AFM images analysis was performed to obtain the line surface R_a (the average deviation of all points roughness profile from a mean line over the evaluation length), RMS surface, R_q (the average of the measured height deviations taken within the evaluation length and measured from the mean line), R_y (the largest single P/V height in five adjoining sampling heights) and R_p maximum peak height (it indicates the point along the sampling length at which the curve is highest). AFM parameters are given in Table 6.

Table 6: AFM data for CS immersed without and with the inhibitor system (line R_a).

Samples	R_a nm	R_q nm	R_y nm	R_p nm
CS surface	33.38	48.77	229.50	142.59
CS immersed in 1 N HCl	342.25	403.34	1611.94	559.73
CS immersed in 1 N HCl + 10% SCLAE	134.56	178.64	745.45	282.12

The table shows that surface R_a for CS in HCl (blank) was very high. With 10% SCLAE, this value decreased, being lower than that for CS in blank HCl, but higher than that for the polished surface. This was due to the protective layer that covered the CS surface. This film was found to be smooth. RMS, maximum P/V height and maximum peak height values also decreased [40-41].

Conclusion

In this study, SCLAE hindered the corrosion of CS immersed in 1 N HCl, with an IE(%) of 91.38%, as verified by WL method. PDP study indicated that the effective SCLAE system functioned predominantly as an anodic inhibitor. Elc impedance measurements showed that, due to the enlarged thickness of the layer adsorbed onto the CS surface, an increase in R_{ct} and a decrease in C_{dl} and I_{corr} values occurred. FTIR spectra revealed that the protective film consisted of a Fe^{2+}-SCL complex. SEM micrographs showed that the inhibited CS surface was like that of the polished one. EDAX analysis gave the constituents on the CS surface. AFM confirmed the CS surface R_a and smoothness. FTIR, SEM, EDAX and AFM analyses revealed that Pc constituents in SCLEA strongly interacted with the CS surface, forming a solid inhibition layer between the substrate and HCl. This film protected CS from HCl further attack.

Authors' contributions

T. Raja: chose the problem; done the literature survey; integrated new ideas with existing literature; completed the experimental part. **S. S. Syed Abuthahir**: helped in the spectral characterization; suggested the interpretation report; guided in the paper writing. **K. Vijaya**: gave outlines for the manuscript preparation.

Acknowledgement

The authors are thankful to the Principal and College Management Committee Members of Jamal Mohamed College (Autonomous), for providing necessary facilities. The authors are also thankful to DBT and DST-FIST, for providing instrumental facilities to carry out research work.

Abbreviations

AC: alternating current
ACIS: alternating current impedance spectroscopy
AFM: atomic force microscopy
C_{dl}: double layer capacitance
CE: counter electrode
CI: corrosion inhibitor/inhibition
CR: corrosion rate
CS: carbon steel
Ct: concentration
E: potential
E_{corr}: corrosion potential
EDAX: energy dispersive analysis of X-rays
Elc: electrochemical
FTIR: Fourier transform infrared
HCl: hydrochloric acid
I: current density
I_{corr}: corrosion current density
IE(%): inhibition efficiency
IT: immersion time
KBr: potassium bromide
LPR: linear polarization resistance values
mdd: milligrams per square decimeter per day
MS: carbon steel
OCP: open circuit potential
Pc: phytochemicals
PDP: potentiodynamic polarization
P/V: peak to valley
R_a: average roughness
R_{ct}: charge transfer resistance
RE: reference electrode
RMS: root-mean-square
SC: saturated calomel
SCL: *Syzygium cumini* leaves

SCLAE: *Syzygium cumini* leaves aqueous extract
SEM: scanning electron microscopy
SPM: scanning probe microscopy
SR: scan rate
T: temperature
WE: working electrode
WL: weight loss

Symbols definition
βa: anodic Tafel slope
βc: cathodic Tafel slope

References

1. Fontana MG, Greene ND. Corrosion Engineering. McGraw-Hill Book Co. New York. 1967.
2. Bergmann JL. Corrosion Inhibitors. New York. 1963.
3. Mohammed A El-Hashemy, Amal S. The inhibitive action of *Calendula officinalis* flower heads extract for mild steel corrosion in 1 M HCl solution. J Mat Res Technol. 2020;9(6):13509-13523. https://doi.org/10.1016/j.jmrt.2020.09.078
4. Khadraoui A, Khelifa A, Hachama K et al. *Thymus algeriensis* extract as a new eco-friendly corrosion inhibitor for 2024 aluminium alloy in 1 M HCl medium. J Mol Liq. 2016;214(2):93-7. https://doi.org/10.1016/j.molliq.2015.12.064
5. Hackerman N. The theory and practice of corrosion and its control in industry. Langmuir. 1987;3:922-924. https://doi.org/10.1021/la00078a009
6. Nathan CC. Organic Inhibitors. NACE. Houston. 1977.
7. Isabel Garcia-santos, Jesus Sanmartin, Ana M Garcia-Deibe et al. Structural and spectroscopic studies on some metal complexes of an 8-hydroxyquinoline derivative. Inorg Chim Acta. 2010;363:193-198. https://doi.org/10.1016/j.ica.2009.09.004
8. Anandan A, Rajendran S, Sathiyabama J et al. Influence of some tablets on corrosion resistance of orthodontic wire made of SS 316L alloy in artificial saliva. Int J Corros Scale Inhib. 2017;6(2):132-141. https://doi.org/10.17675/2305-6894-2017-6-2-3
9. Arjun G, Kalkhambkar SK, Rajappa BM et al. *Saussurea obvallatta* leaves extract as a potential eco-friendly corrosion inhibitor for mild steel in 1 M HCl. Inorg Chem Comm. 2022;143(2-3);109799. https://doi.org/10.1016/j.inoche.2022.109799
10. Manohar R, Rathod RL, Minagalavar S et al. Effect of *Artabotrys odoratissimus* extract as an environmentally sustainable inhibitor for mild steel corrosion in 0.5 M H_2SO_4 media. J Indian Chem Soc. 2022;99(5);100445. https://doi.org/10.1016/j.jics.2022.100445
11. Manohar R, Rathod RL, Rajappa BM et al. Investigation of *Dolichandra unguiscati* leaves extract as a corrosion inhibitor for mild steel in acid medium. Curr Res Green Sust Chem. 2021;4;100113. https://doi.org/10.1016/j.crgsc.2021.100113
12. Gunavathy N, Murugavel SC. Corrosion inhibition of mild steel in acid medium using MUSA *Acuminata flower* extract. J Environ Nanotechnol. 2013;2(4):45-50. https://doi.org/10.1155/2012/952402
13. El Bribri A, Tabyaoui M, Tabyaoui B et al. The use of *Euphorbia falcata* extract as eco- friendly corrosion inhibitor of carbon steel in hydrochloric acid solution. Mater Chem Phys. 2013;141(1):1-7. https://doi.org/10.1016/j.matchemphys.2013.05.006

14. Mourya P, Banerjee S, Singh MM. Corrosion inhibition of mild steel in acidic solution by *Tagetes erecta* (Marigold flower) extract as a green inhibitor. Corros Sci. 2014;85(3):52-63. https://doi.org/10.1016/j.corsci.2014.04.036
15. Li L, Zhang X, Lei J et al. Adsorption and corrosion inhibition of *Osmanthus fragran* leaves extract on carbon steel. Corros Sci. 2012;63:82-90. https://doi.org/1016/j.corsci.2012.05.026
16. Rajendran A. Isolation, characterization, pharmacological and corrosion inhibition studies of flavonoids obtained from *Nerium oleander* and *Tecoma stans*. Int J Pharm Technol Res. 2011;3(2):1-13.
17. Mohammed A El-Hashemy, Amal Sallam. The inhibitive action of *Calendula officinalis* flower heads extract for mild steel corrosion in 1 M HCl solution. J Mater Res Technol. 2020;9(6):13509-13523. https://doi.org/10.1016/j.jmrt.2020.09.078
18. Gunavathy S, Murugavel S. Corrosion inhibition studies of mild steel in acid medium using *Musa acuminate* fruit peel extract. E-J Chem. 2012; 9(1):487-495. https://doi.org/10.1155/2012/952402
19. Mohammed Al Hashemy, Amal Sallam. The inhibitive action of *Calendula officinalis* flower heads extract for mild steel corrosion in 1 M HCl solution. J Mater Res Technol. 2020;9(6):13509-13513. https://doi.org/10.1016/j.jmrt.2020.09.078
20. Yaro AS, Wael RK, Khadom AA et al. Reaction kinetics of corrosion of mild steel in phosphoric acid. J Univ Chem Technol Metallur. 2010;45(4):443-448.
21. Syed Abuthahir SS, Jamal Abdul Nasser A, Rajendran S. Inhibition effect of copper complex of 1-(8-Hydroxy quinolin-2yl-methyl) thiourea on the corrosion of mild steel in a sodium chloride solution. Open Mater Sci. 2014;8(1):71-80. https://doi.org/10.2174/1874088X01408010071
22. Nazeera Banu VR, Rajendran S, Syed Abuthahir SS. Corrosion Inhibition by Self-assembling Nano films of Tween 60 on Mild steel surface. Int J Chem Concepts. 2017;3(1):161-173.
23. Karthik K, Selvaraj SK, Pandeeswaran M et al. Synergistic corrosion inhibition effect of carbon steel in sea water by hydroxy Proline - Zn^{2+} System. Int J Adv Chem Sci Appl. 2015;3(4):54-59.
24. Fabrizio Zucchi, Ibrahim Hashi Omar. Plant extracts as corrosion inhibitors of mild steel in HCl solutions. Surf Technol. 1985;24(4):391-399. https://doi.org/10.1016/0376-4583(85)90057-3
25. Samsath Begum A, Jamal Abdul Nasser A, Mohamed Kasim Sheit H et al. *Abrus precatorius* leaf aqueous extract as a corrosion inhibitor on mild steel in 1.0 M HCl solution. Int J Basic Appl Res. 2019;9(2):438-450.
26. Tuama RJ, Al-Dokheily ME, Khalaf MN. Recycling and evaluation of poly (ethylene terephthalate) waste as effective corrosion inhibitors for C-steel material in acidic media. Int J Corros Scale Inhib. 2020;9(2):427-445. https://doi.org/10.17675/2305-6894-2020-9-2-3
27. Jeeva PA, Mali GS, Dinakaran R et al. The influence of Co-Amoxiclav on the corrosion inhibition of mild steel in 1 N hydrochloric acid solution. Int J Corros Scale Inhib. 2019;8(1):1-12. https://doi.org/10.17675/2305-6894-2019-8-1-1
28. Shanthy P, Thangakani JA, Karthika S, et al. Corrosion inhibition by an aqueous extract of *Ervatamia divaricate*. Int J Corros Scale Inhib. 2021;10(1):331-348. https://doi.org/10.17675/2305-6894-2021-10-1-19
29. Barrahi M, Elhartiti H, El Mostaphi A et al. Corrosion inhibition of mild steel by Fennel seeds mill (*Foeniculum vulgare*) essential oil in 1 M hydrochloric acid solution. Int J Corros

Scale Inhib. 2019;8(4):937-953. https://doi.org/10.17675/2305-6894-2020-10-4-10
30. Mahalakshmi P, Rajendran S, Nandhini G et al. Inhibition of corrosion of mild steel in sea water by an aqueous extract of turmeric powder. Int J Corros Scale Inhib. 2020;9(2):706-725. https://doi.org/10.17675/2305-6894-2020-9-2-20
31. Ikhmal WMK, Yasmin MYN, Mari MFF et al. Evaluating the performance of *Andrographis paniculata* leaves extract as additive for corrosion protection of stainless steel 316L in sea water. Int J Corros Scale Inhib. 2020;9(1):118-133. https://doi.org/10.17675/2305-6894-2020-9-1-7
32. Grace Baby A, Rajendran S, Johnsirani V et al. Influence of zinc sulphate on the corrosion resistance of L80 alloy immersed in sea water in the absence and presence of sodium potassium tartrate and trisodium citrate. Int J Corros Scale Inhib. 2020;9(3):979-999. https://doi.org/10.17675/2305-6894-2020-9-3-12
33. Rajendran S, Srinivasan R, Dorothy R et al. Green solution to corrosion problems – at a glance. Int J Corros Scale Inhib. 2019;8(3):437-479. https://doi.org/10.17675/2305-6894-2019-8-3-1
34. Peter A, Sharma SK. Use of *Azadirachta indica* (AZI) as green corrosion inhibitor against mild steel in acidic medium: anti-corrosive efficacy and adsorptive behavior. Int J Corros Scale Inhib. 2017;6(2):112-131. https://doi.org/10.17675/2305-6894-2017-6-2-2
35. Dehghani A, Bahlakeh G, Ramezanzadeh B et al. Potential role of a novel green eco-friendly inhibitor in corrosion inhibition of mild steel in HCl solution: Detailed macro/micro-scale experimental and computational explorations. Constr Build Mat. 2020;245:118464. https://doi.org/10.1016/j.conbuildmat.2020.118464
36. Kıcır N, Tansu˘ G, Erbil M et al. Investigation of ammonium (2, 4-dimethylphenyl)-dithiocarbamateas a new effective corrosion inhibitor for mild steel. Corros Sci. 2016;105:88-99. https://doi.org/10.1016/j.corsci.2016.01.006
37. Verma C, Ebenso EE, Bahadur I et al. An overview on plant extracts as environmental sustainable and green corrosion inhibitors for metals and alloys in aggressive corrosive media. J Mol Liq. 2018;266:577-590. https://doi.org/10.1016/j.molliq.2018.06.110.
38. Karthikeyan S, Syed Abuthahir SS, Samsath Begum A et al. Corrosion Inhibition of Mild Steel in 0.5 M H2SO4 Solution by Plant Extract of *Annona squamosal*. Asian J Chem. 2021;33(9):2219-2228. https://doi.org/10.14233/ajchem.2021.23386
39. Li L, Xueping Z, Jinglei L et al. Adsorption and corrosion inhibition of *Osmanthus fragran* leaves extract on carbon steel. Corros Sci. 2012;5:1-26. https://doi.org/10.1016/j.corsci.2012.05.026
40. Arjun G, Kalkhambkar SK, Rajappa BM. Effect of Schiff bases on corrosion protection of mild steel in hydrochloric acid medium: Electrochemical, quantum chemical and surface characterization studies. Chem Eng J Adv. (2022);12:100407. https://doi.org/10.1016/j.ceja.2022.100407
41. Manohar R, Rajappa MB, Kittur AA. *Garcinia livingstonei* leaves extract influenced as a mild steel efficient green corrosion inhibitor in 1 M HCl solution. Mat Today: Proceed. 2022;54:786-796. https://doi.org/10.1016/j.matpr.2021.11.084